Mesoscale Barotropic Instability of Vortex Rossby Waves in Tropical Cyclones

ZHONG Wei*[1] (钟 玮), LU Han-Cheng[1] (陆汉城), and Da-Lin ZHANG[2]

[1]*Institute of Meteorology, PLA University of Science and Technology, Nanjing* 211101

[2]*Department of Atmospheric and Oceanic Science, University of Maryland, College Park, Maryland* 20742, *USA*

ABSTRACT

In this study, the barotropic stability of vortex Rossby waves (VRWs) in 2D inviscid tropical cyclone (TC)-like vortices is explored in the context of rotational dynamics on an f-plane. Two necessary instable conditions are discovered: (a) there must be at least one zero point of basic vorticity gradient in the radial scope; and (b) the relative propagation velocity of perturbations must be negative to the basic vorticity gradient, which reflects the restriction relationship of instable energy. The maximum growth rate of instable waves depends on the peak radial gradient of the mean vorticity and the tangential wavenumber (WN). The vortex-semicircle theorem is also derived to provide bounds on the growth rates and phase speeds of VRWs.

The typical basic states and different WN perturbations in a tropical cyclone (TC) are obtained from a high resolution simulation. It is shown that the first necessary condition for vortex barotropic instability can be easily met at the radius of maximum vorticity (RMV). The wave energy tends to decay (grow) inside (outside) the RMV due mainly to the negative (positive) sign of the radial gradient of the mean absolute vorticity. This finding appears to help explain the developemnt of strong vortices in the eyewall of TCs.

Key words: vortex Rossby waves, vortex barotropic instability, vortex semicircular theorem, tropical cyclone

1. Introduction

Recent advances in radar meteorology and rapid growth in computer power have generated many observational and modeling studies showing different meso- and small-scale structures in the inner-core regions of tropical cyclones (TCs), such as small-scale vortices, spiral rainbands and the polygonal eyewall. These asymmetrical features, evolving over a timescale ranging from a few minutes to hours, may lead to rapid changes in TC intensity and path. Therefore, understanding the generation and propagation of the asymmetric features could reveal their roles in the structural and intensity changes of TCs and improve our knowledge of TC dynamics.

A TC can be viewed as a highly symmetrical vortex with deep moist convective motion so that a 2D axi-symmetrical model (e.g. Eliassen, 1952; Emanuel, 1995) in a radial height plane can represent approximately its evolving circulation. So many earlier studies have attributed the development of spiral rainbands to the outward propagation of internal inertial gravity waves (IGWs) (e.g. Tepper, 1958; Willoughby, 1978a, b; Xu, 1982). However, internal IGWs often propagate at speeds that are much faster than those of spiral rainbands, based on radar observations. Thus, research interests have shifted, since the 1990s, to the vortex Rossby wave (VRW) theory of MacDonald (1968), who suggested that spiral rainbands were "Rossby-like" waves possessing a counter-gradient momentum flux.

By invoking an analogy between radial gradients of the basic state absolute vorticity in TCs and meridional gradients of the planetary vorticity in large-scale weather systems, Montgmery and Kallenbach (1997) advanced the VRW theory by obtaining the following local dispersion relation of radially and azimuthally propagating VRWs at a certain radius r_0 from the non-

*Corresponding author: ZHONG Wei, vivian.zhongwei@gmail.com

divergent barotropic vorticity equation:

$$\omega_R = n\overline{\Omega}_0 + \frac{nd\bar{\eta}_0/dr}{r_0(l^2 + n^2/r_0^2)} \ ,$$

where $\overline{\Omega}_0$ and $d\bar{\eta}_0/dr$ are the mean angular velocity and mean radial absolute vorticity gradient at $r = r_0$, respectively; and l and n are the radial and azimuthal WNs. Because its phase velocity is close to that of spiral rainbands, the VRW theory has been widely used to explain the structural changes and evolution of the eyewall and spiral raindbands in TCs (e.g. Montgomery and Franklin, 1998; Montgomery and Franklin, 1998; Schecter and Montgomery, 2007).

Because the basic state of a TC can be viewed as a symmetric vortex system with a "slow manifold" feature of balanced flows, the VRW theory, in which divergence is assumed much weaker than rotation, has been used to describe the perturbation feature of low WN waves on the basic vortex and, and it could to some extent explain the structural changes of the asymmetric eyewall and spiral rainbands. Reasor et al. (2000) examined the low WN asymmetric structure and evolution of Hurricane Olivia's (1994) inner core through airborne dual Doppler radar with a 30-min time resolution for 3.5 hours, during which period the hurricane experienced a weakening. The authors found that the vorticity bands in the TC were characterized by VRWs and might contribute to the observed rainbands with a similar radial wavelength. Recent simulation research has also demonstrated the existence of VRWs in the core region of TC like vortices (Wang, 2002a, b).

The growth of disturbances associated with barotropic and baroclinic instability of the symmetrical hurricane vortex has for some time been argued as a cause of such phenomena as polygonal eyewalls, mesocyclone formation, and possibly even supercells in and near hurricane eyewalls (Schubert et al., 1999). Working in the context of plasma physics, Smith and Rosenbluth (1990) discovered an exact closed-form solution, in terms of quadratures, describing the evolution of linearized azimuthal WN-1 disturbances on inviscid 2D vortices. Rezink and Dewar (1994) showed there can be no exponentially unstable modes in a 2D inviscid vortex for WN-1 with linear theory, whereas Smith and Rosenbluth (1990) demonstrated that the long-term asymptotic behavior of their exact solution could exhibit linear growth in wave energy, The necessary and sufficient requirement for growth in this solution is the existence of at least one local maximum in the angular velocity of the basic state swirling flow, other than at the circulation center. An associated asymptotic result for zero total circulation vortices in unbounded domains was found by Llewellyn Smith (1995). Based on the work of Smith and Rosenbluth (1990), Nolan and Montgomery (2000) studied the dynamics of this algebraic instability in the near-core area of hurricanes.

The next section shows how the necessary conditions for barotropic instability in a hurricane-like vortex are deduced. The semi-circle theorem providing bounds on the growth rates and wave phase speeds will also be presented. Section 3 provides diagnoses of barotropic instability of VRWs using a high-resolution cloud-resolution simulation of Hurricane Andrew (1992). The upper bound of the barotropic growth rate of VRWs and the optimum WN for the most unstable waves will be discussed, too. A summary and concluding remarks are given in the final section.

2. Barotropic instability of vortex Rossby waves

To discuss the instability feature of VRWs on 2D inviscid vortices at the approximation of the f-plane, we start from the linear barotropic vorticity equation, as follows (Montgmery and Kallenbach, 1997):

$$\left(\frac{\partial}{\partial t} + \frac{\overline{V}}{r}\frac{\partial}{\partial \lambda}\right)\tilde{\zeta} + \tilde{u}\frac{d\bar{\eta}}{dr} = 0 \ , \tag{1}$$

where $\tilde{u}$ and $\tilde{v}$ are radial and tangential wind perturbation, respectively; $\overline{V}(r)$ is the mean tangential wind; $\bar{\eta} = f + 2\overline{\Omega} + rd\overline{\Omega}/dr$ is the mean absolute vorticity; $d\bar{\eta}/dr$ is the radial gradient of the mean absolute vorticity, which is analogous to the β-effect in the classic Rossby wave theory; and $\tilde{\zeta} = \partial r\tilde{v}/r\partial r - \partial \tilde{u}/r\partial \lambda$ denotes perturbation vorticity. Assuming that the horizontal perturbation divergence is much smaller than perturbation vorticity in the barotropic vorticity equation, the perturbation streamfunction, $\tilde{\psi}$, can be introduced as:

$$\tilde{u} = -\frac{\partial \tilde{\psi}}{r\partial \lambda} \ , \qquad \tilde{v} = \frac{\partial \tilde{\psi}}{\partial r} \ . \tag{2}$$

On the basis of Montgomery and Kallenbach's (1997) wave analyzing method, the time change of the wave is considered to be neglectable. Then, by taking account of the particularity of perturbation at the TC eye and boundary radius, we can assume that the spatial and temporal dependence of $\tilde{\psi}$ may be separated by specifying solutions in the form of azimuthally propagating waves:

$$\tilde{\psi}(r, \lambda, t) = \psi(r)\exp[i(k\lambda - \omega t)] \ , \tag{3}$$

where $\psi(r)$ is the wave amplitude of perturbation streamfunction, k is the tangential WN, and ω is the local wave frequency at $r = r_0$. Because the radial length scale of the waves is much smaller than the characteristic radius of a TC vortex, some basic state

variables may be assumed to be slowly varying and expanded in series (Montgmery and Kallenbach, 1997). That is,

$$
\begin{cases}
\overline{V} = \overline{V}_0 + \overline{V}'_0 \Delta r + \cdots \\
\dfrac{d\bar{\eta}}{dr} = \bar{\eta}'_0 + \bar{\eta}''_0 \Delta r + \cdots \\
\dfrac{1}{r} = \dfrac{1}{R}\left(1 - \dfrac{\Delta r}{R} + \cdots\right)
\end{cases}, \qquad (4)
$$

where $\Delta r = r - r_0$. The superscript of' ($''$) denotes the first-(second-) order derivative; and R is the value of r_0. By substituting Eqs. (2) and (4) into Eq. (1), and neglecting high-order small variables and introducing that $\omega = kc/R$, we obtain the following linearized barotropic vorticity equation for perturbation streamfunction:

$$
\left(\overline{V}_0 - c\right)\left(\frac{1}{R}\psi' + \psi'' - \frac{k^2}{R^2}\psi\right) - \bar{\eta}'_0\psi = 0, \qquad (5)
$$

where c is the propagation velocity of waves.

2.1 Necessary conditions for vortex barotropic instability

According to the classical theory and method of barotropic instability, we discuss the first barotropic instability requirement in advance. Substituting the expression of wave velocity and amplitude into Eq. (5) (defined as $c = c_r + ic_i$, $\psi = \psi_r + i\psi_i$), the real and imaginary parts of the equations can be obtained:

$$
\psi''_r + \frac{1}{r}\psi'_r - \frac{k^2}{r^2}\psi_r - \frac{\left(\overline{V}_0 - c_r\right)\bar{\eta}'_0}{\left(\overline{V}_0 - c_r\right)^2 + c_i^2}\psi_r +
$$
$$
\frac{c_i\bar{\eta}'_0}{\left(\overline{V}_0 - c_r\right)^2 + \omega_i^2}\psi_i = 0, \qquad (6)
$$

$$
\psi''_i + \frac{1}{r}\psi'_i - \frac{k^2}{r^2}\psi_i - \frac{\left(\overline{V}_0 - c_r\right)\bar{\eta}'_0}{\left(\overline{V}_0 - c_r\right)^2 + c_i^2}\psi_i -
$$
$$
\frac{c_i\bar{\eta}'_0}{\left(\overline{V}_0 - c_r\right)^2 + \omega_i^2}\psi_r = 0. \qquad (7)
$$

where the subscript of $r(i)$ denotes the real (imaginary) part of variables.

By taking ψ_iEq. (6)$-\psi_r$Eq. (7), the above real and imaginary parts of the barotropic equations can be joined as:

$$
\left(R\psi_i\psi'_r - R\psi_r\psi'_i\right)' = -\frac{Rc_i\bar{\eta}'_0}{\left(\overline{V}_0 - c_r\right)^2 + c_i^2}(\psi_i^2 + \psi_r^2). \qquad (8)
$$

The associated boundary conditions are:

$$
\left.\frac{\partial \psi'}{\partial \lambda}\right|_{R=0} = 0, \qquad \left.\frac{\partial \psi'}{\partial \lambda}\right|_{R=R_b} = 0, \qquad (9)
$$

in which R_b is the radius at the outermost boundary. Furthermore, with the restriction of barotropic boundary conditions and the support of Rolle's Theorem, there must exist at least one point defined as R_k, which satisfies:

$$
-\frac{c_i\bar{\eta}'_0}{\left(\overline{V}_0 - c_r\right)^2 + c_i^2}(\psi_i^2 + \psi_r^2)|_{R=R_k} = 0. \qquad (10)
$$

As the definition of instability requires that the imaginary part of wave velocity and streamfunction cannot be zero, that is $c_i \neq 0, \psi_i \neq 0$, from the previous formula there must be:

$$
\bar{\eta}'_0\big|_{R=R_k} = 0, \qquad (11)
$$

which is the first necessary requirement of mesoscale barotropic instability for vortex Rossby waves. Similar to the classic barotropic instability theorem (Kuo and Zhu, 1981) for Rossby waves, the necessary requirement to make the vortex Rossby wave instable is that, within the boundary of the TC, there must exist at least one point at which the radial gradient of basic absolute vorticity is zero. This requirement provides the necessary conditions for background fields of the TC.

It is important to note that Eq. (11) only provides a necessary condition for barotropic instability of VRWs, whether or not they amplify would depend on their perturbation kinetic energy. To see this, integrating the sum of ψ_rEq. (6)$+\psi_i$Eq. (7) from $R = 0$ to $R = R_b$, and substituting the boundary conditions lead to the integral equation of perturbation kinetic energy:

$$
\int_0^{R_b} RE_p dR = -\int_0^{R_b} \frac{R(\overline{V}_0 - c_r)\bar{\eta}'_0}{\left(\overline{V}_0 - c_r\right)^2 + c_i^2}\left(\psi_r^2 + \psi_i^2\right) dR, \qquad (12)
$$

where

$$
E_p = \frac{1}{2}(u'^2 + v'^2) = |\psi'|^2 + \frac{k^2}{R^2}|\psi|^2,
$$

denotes the total perturbation kinetic energy. Because the perturbation kinetic energy must be expected to increase with time for unstable VRWs, i.e. $E_p > 0$, it is evident from Eq. (12) that we must have:

$$
\left(\overline{V}_0 - c_r\right)\bar{\eta}'_0 < 0. \qquad (13)
$$

Since the VRWs discussed herein propagate azimuthally with respect to the mean tangential flows, we may denote $\overline{V}_0 - c_r$ as the relative propagation velocity with respect to the mean rotational flows. Then, Eq. (13) implies that if the wave energy grows with time, the relative propagation velocity and the radial gradients of the basic-state absolute vorticity must be negatively correlated; this represents the second necessary condition for vortex-barotropic instability.

2.2　The maximum growth rate and vortex semicircle theorem

After obtaining the two necessary conditions for barotropical instability, the growth rate of VRWs can be estimated from the real part of solutions. Specifically, given the boundary conditions Eq. (9), $\psi(R)$ can be expanded with a finite Fourier sine series like:

$$\psi(R) = \sum_{n=1}^{\infty} a_n \sin \frac{n\pi R}{R_{\mathrm{b}}} , \qquad (14)$$

where $a_n (n=1, 2, 3, \dots)$ are real coefficients. Substituting this Fourier progression into Eq. (12), and taking the upper bound of instability growth rate as the maximum possible growth rate (MPGR), denoted as $\omega_{i\,\max}$, the growth rate of barotropic VRWs can be estimated as (Appendix A):

$$\frac{k\,|c_i|}{R} \leqslant \omega_{i\,\max} = \frac{k}{2R\,(\pi^2 + k^2)} \max_{(0, R_{\mathrm{b}})} (|\bar{\eta}'_0|) . \quad (15)$$

It is obvious from Eq. (15) that vortex barotropic instability will not occur at all WNs, but it is more scale-selective, which is similar to that for the classic barotropic instability. In particular, the growth rate has an upper bound that depends on the maximal radial gradient of basic-state vorticity. The distribution of the MPGR as a function of azimuthal WN is given in Fig. 1, which shows that when $k \to 0$ or $k \to \infty$, $\omega_{i\,\max} \to 0$. But the growth rate reaches the MPGR at $k = 3$, indicating that the most unstable VRW occurs near WN-3.

As mentioned before, the phase velocity of VRWs has important influences on barotropic wave stability. This can be more clearly seen from the vortex-semicircle theorem. Let us start from a transformation on an f-plane by letting

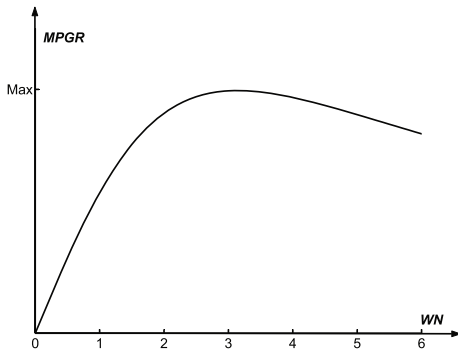$$F = \frac{\psi}{\overline{V} - c} . \qquad (16)$$

Fig. 1. Maximum possible growth rate of instable waves.

Taking the above expression and adopting the f-plane approximation, and multiplying the above equation by F^*, the complex conjugate of F, Eq. (7) can be changed into:

$$\left[R(\overline{V}_0 - c)^2 F^* F'\right]' + \frac{\overline{V}_0^2}{R}(\overline{V}_0 - c)\,|F|^2 - $$
$$R(\overline{V}_0 - c)^2 \left[\frac{k^2}{R^2}\,|F|^2 + |F'|^2\right] = 0 . \quad (17)$$

Suppose that $\overline{V}_{\min}$ and $\overline{V}_{\max}$ are the minimum and maximum of basic tangential wind speed at $(0, R_b)$, and $\overline{\Omega}_{\max}$ is the corresponding maximum basic angular velocity, we may estimate c_r as:

$$\overline{V}_{\min} - \frac{R_{\mathrm{b}}^2 \overline{\Omega}_{\max}^2}{2\,(\pi^2 + k^2)} \leqslant c_r \leqslant \overline{V}_{\max} ; \qquad (18)$$

which gives the bounds for the phase velocity of amplifying VRWs. Clearly, unstable waves cannot propagate at or larger than the maximum speed of the mean flow. The corresponding relationship in complex plane can be written as

$$(c_r - U)^2 + c_i^2 \leqslant c_R^2 , \qquad (19)$$

where

$$U = (\overline{V}_{\max} + \overline{V}_{\min})/2 ,$$
$$c_R^2 = U^2 + u\overline{\Omega}_{\max}^2 R_{\mathrm{b}}^2 / \left(\pi^2 + k^2\right) ,$$

and

$$u = (\overline{V}_{\max} - \overline{V}_{\min})/2$$

(see Appendix B for more detailed derivations). Equation (19) indicates that the complex eigenvalue, $c = c_r + ic_i$, must lie within the circle centered at $[U, 0]$ in the complex plane with a radius of c_t. Longer VRWs tend to have larger ranges for dynamical instability. Because we are interested in unstable modes, i.e., c_i is positive, only the upper half of the circle is relevant, as given in Fig. 2. From the analysis of the figures, we know that: (1) when $c_r = U \pm c_R$ $(c_R > 0)$, then $c_i = 0$, which means in the range of the semicircle the waves which propagate fastest or slowest are stable; (2) when $c_r = U$, the instable growth rate reaches its extreme, and the value is $c_i = c_R$. That is the vortex semicircular theorem of barotropic vortex Rossby wave instability.
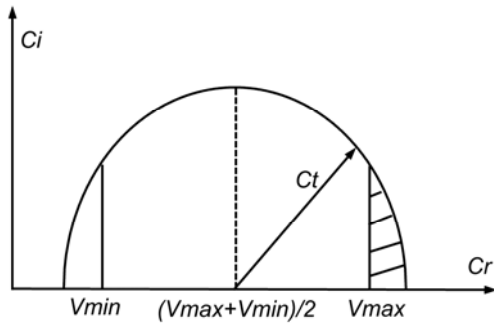
Fig. 2. Sketch map of vortex semicircular theorem for barotropic instability. c_t denotes the phase speed at maximum radius in complex plane of wave volocity.

3. Mesoscale barotropic instability in a simulated TC

In this section, we apply the vortex-barotropic instability theory discussed in the preceding section to a successful cloud-resolving simulation of Hurricane Andrew (1997) (Liu et al., 1997, 1999). Ideally speaking, in the study of any dynamical instability, especially with linear equations, the basic state must satisfy exactly the equations system used to derive the associated stability criterion. There are two basic requirements for the application of the instability theory: barotropic flows and dynamical consistency among dynamical variables. Although there are strong inflows and outflows at the low and high levels, respectively, Anthes (1982) divided a TC vortex into four dynamic areas, and pointed out that the midlevel flows can be regarded approximately as barotropic. In the present case, the barotropic conditions can be obtained by considering the azimuthally-averaged midlevel flows of the simulated Andrew at a timescale that is much longer than that of the wave instability (Liu et al., 1997, 1999). As for the second requirement, the simulation data, exhibiting many typical structures of TCs, has been shown to be dynamically consistent among different flow fields (Zhang et al., 2000, 2001, 2002). Therefore, the model-simulated variables are azimuthally and vertically averaged in the 900–800 hPa layer, followed by 3-hour temporal averages during the mature stage of Andrew in order to obtain more representative basic-state quantities of the storm for the application of vortex-barotropic instability theory.

3.1 *Diagnosis of the necessary conditions*

The radial distribution of basic tangential wind, $\overline{V}$, in Fig. 3a, shows that the maximum tangential wind of TC Andrew (1992) exceeded 70 m s^{-1}, with an RMW of 40 km. It is shown that the simulated basic angular velocity and vertical absolute vorticity are in marked contrast to a hypothetical near-Gaussian swirl profile

with the maximum rotation at the TC center (Montgmery and Kallenbach, 1997) (Figs. 3b and c). The basic angular velocity is very small in the hurricane eye and quickly increscent with the basic tangential wind when approaching the RMW. After reaching its maximum at the RMW (marked by R_w in Fig. 3), the basic angular velocity becomes attenuating in the outer area (Fig. 3b). The radial distribution of basic absolute vorticity, $\bar{\eta}$, is the same with basic angular velocity, which reaches its maximum at the RMV (R_k), inside of the RMW, and is damped to the two poles of the eye and the outer region of the TC. This distribution is in accordance with three basic states from a vortex modeled after an intense (category three) hurricane, a moderate (category one) hurricane, and a weak tropical storm (Nolan and Montgomery, 2002). Meanwhile, as the decisive factor in the formation and propagation of vortex Rossby waves, the structure of the radial gradient of basic absolute vorticity, $\bar{\eta}'$, is also crucial to the instability of waves. It is evident from Fig. 3d that the radial gradient of the basic state absolute vorticity is zero at the RMV, at which point the first necessary condition for barotropic instability is met.

Since $\bar{\eta}'_0 > 0$ ($\bar{\eta}'_0 < 0$) inside (outside) the RMV within (R_k, R_b), the second necessary condition requires that if unstable waves can intensify inside the RMV, there must have $\overline{V}_0 - c_r < 0$. In other words, when the phase speed of VRWs exceeds the basic flows, it may cause the instable development of perturbation. The theoretical velocity of vortex Rossby waves estimated by Montgmery and Kallenbach (1997) is on the order of magnitude of 10^{-1}–10^0 m s^{-1}, which is far slower than the simulated tangential wind. This indicates that propagating VRWs may not be able to amplify inside the RMV or the calm eye. On the other hand, in the outer region, $\bar{\eta}' < 0$, the second necessary condition requires $\overline{V}_0 - c_r > 0$. Since the phase velocity of VRWs is much slower than the mean tangential flows, the second necessary condition can be easily met. This suggests that the outer region is more favorable than the inner region for the amplification of propagating VRWs. Based on the above analysis, we may state that the existence of the RMW and RMV provides the first necessary condition for vortex barotropic instability, while the sign of the radial gradient in the absolute vorticity indicates propagating VRWs may (may not) amplify outside (inside) the RMV.

3.2 *The perturbation structure of different WNs*

In this section, the method of asymmetric Fourier wave decomposition is performed to further understand the distribution of asymmetries in the inner core
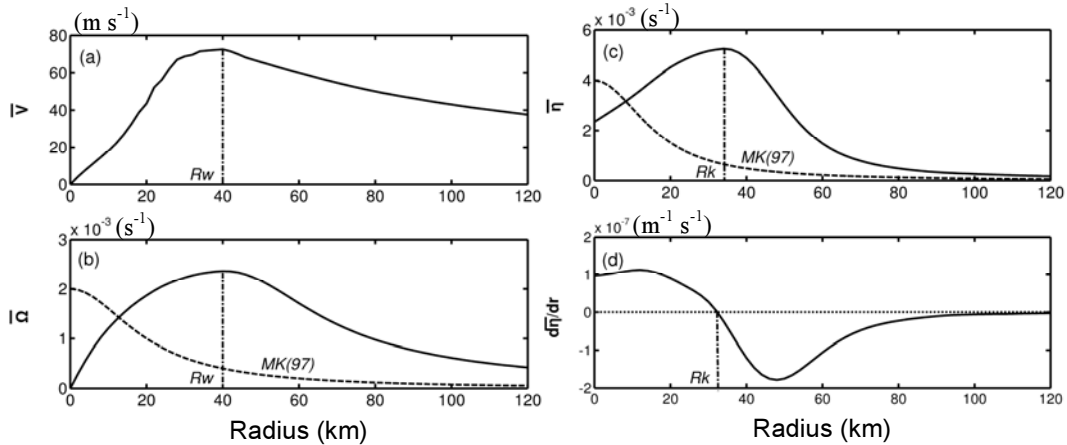
Fig. 3. Basic state radial profiles of Hurricane Andrew (1992) with the finest grid size of 2 km: (a) tangential wind ($\overline{V}$, m s^{-1}); (b) angular velocity ($\overline{\Omega}$, s^{-1}); (c) vertical absolute vorticity ($\bar{\eta}$, s^{-1}), and (d) its radial gradient ($d\bar{\eta}/dr$, m^{-1} s^{-1}). Dashed lines in (b) and (c) show the swirl profile of basic angular velocity and vertical absolute vorticity (Montgomery and Kallenbach, 1997). Dot-dashed lines in (b) and (c) denote the RMW (R_w) and RMV (R_k), respectively.
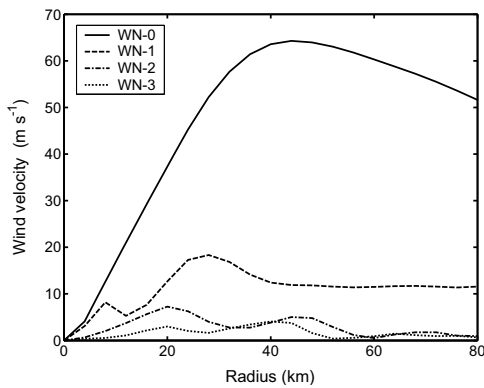

Fig. 4. Radial distribution of WN-0 (solid line), WN-1 (dashed line), WN-2 (dot-dashed line), and WN-3 (dotted line) components of wind velocity (m s^{-1}) at 850 hPa, obtained by averaging three model outputs at 20-min intervals during a 1-hour period at 0000 UTC 24 August 1992.

of the TC, especially the mesoscale deep moist convections in the eyewall. It is given that all the variables can be divided as:

$$P = P_0 + \sum_k P_k,$$

where P_0 is the symmetric component and P_k is the asymmetric component with WN k. The radial distribution of WN-0, WN-1, WN-2, and WN-3 components of wind velocity at 850 hPa are shown in Fig. 4. Obviously, the perturbation wind components are about one order of magnitude smaller than the azimuthal mean in the inner core region. Moreover, the higher the WN, the smaller the magnitude of perturbation winds. These results are similar to those of

Wang and Zhang (2003), and conform to the observational findings of Reasor et al. (2000). Anatomizing their features in the inner core region, we find that the WN-1 component of perturbation wind is the main component of asymmetric wind amplitude and its peak locates between the RMV and RMW. After mild attenuation with the radius, it remains at a magnitude of about 10^1. Both the WN-2 and WN-3 components have two peaks respectively around the RMV and RMW, and their amplitude sharply decreases in the outer region. According to the above analysis of barotropic instability, it is shown that the zero point of the radial gradient of absolute vorticity at the RMV and the strong tangential wind at the RMW provides advantageous dynamic conditions to excite and maintain the development of perturbation.

The horizontal structures of perturbation height and flow vectors, which are obtained by averaging three model outputs at 20-min intervals during a 1-hour period at 0000 UTC 24 August 1992, are given in Fig. 5. It is shown that the WN-1 perturbation height is symmetrical to the TC eye, and the positive and negative extreme centers extend from the RMV to the outside of the RMW, which superposes the area of mesoscale barotropic instability with a large instability growth rate. We can include the fact that the intense development of severe storms in the eyewall has a close relationship with mesoscale barotropic instability. The configuration of perturbation height and wind basically satisfies a balanced relationship, which means the low (high) perturbation height center corresponds to the cyclonic (anti-cyclonic) flow, denoting the feature of vortex Rossby waves. However, there exist distinct unbalanced perturbation winds travers-
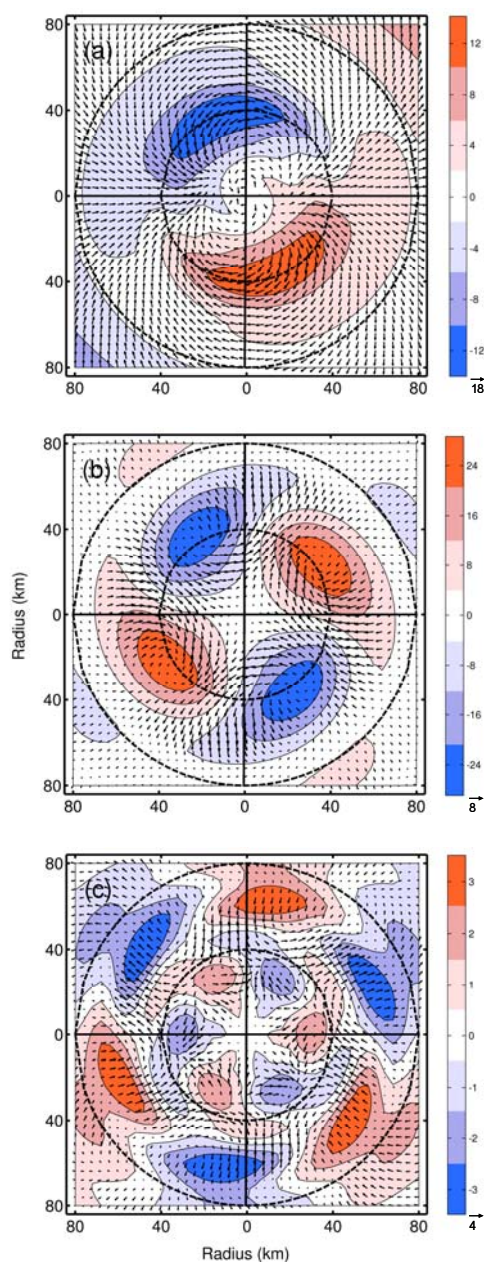
Fig. 5. Horizontal structures of perturbation height (solid lines with shading, m) and flow vectors (m s^{-1}), associated with (a) WN-1, (b) WN-2, and (c) WN-3 components. (Simulation data used here was the same as used for Fig. 4).

ing the isohypses around the RMV, as well as between the high and low perturbation height center. Furthermore, when approaching the outer region of the TC, unlike the theoretical wave structure of pure VRWs (Montgmery and Kallenbach, 1997), there are also strong perturbation heights and unbalanced radial wind, denoting the feature of gravity waves. So, recent research has shown that with the coexistence of rota-

tion and divergence in the TC, the tangential propagation waves will show the mixed feature of VRWs and gravity waves.

The perturbation height centers of WN-2 mainly locate around the RMW. According to the estimate of MPGR, the radial perturbation wind and perturbation height associated with the unbalanced radial wind is obviously larger than that of WN-1. Mostly, WN-3 perturbation wind is radial wind and its perturbation height centers appear in the outer region of the RMW with a distinct radial distribution.

4. Summary and concluding remarks

It is known that the structure and propagation of waves determine the evolution of perturbation on basic flows and that the instability state of waves exert an essential influence on the configuration and intensity changes of the atmospheric system through the growing (or attenuation) of perturbation and its reciprocity with basic flows. Based on the dynamic framework of a 2D non-divergent inviscid vortex system on an f-plane, the barotropic instability of vortex Rossby waves has been discussed. Two necessary instable conditions were discovered: first, that there must be at least one zero point of basic vorticity gradient in the radial scope; and second, that relative propagation velocity of perturbations must be negative to the basic vorticity gradient, which ensures the growth of instable energy.

Furthermore, the instable waves cannot be infinitely increasing. The maximum possibility upper bound of growth rate is deduced to be

$$\frac{k}{2R\left(\pi^2 + k^2\right)} \max_{(0,R_{\mathrm{b}})}\left(|\bar{\eta}_0'|\right) \ ,$$

whose maximum value is at WN-3. According to the vortex semicircular theorem of barotropic vortex Rossby wave instability, the local instable waves have selectivity to their own phase velocity in the complex plane. The possible value range radius of complex phase speeds of instability is related to the basic state as well as WN. In the range of the semicircle, the waves which propagate fastest or slowest are stable, and when $c_r = (\overline{V}_{\max} + \overline{V}_{\min})/2$, the instable growth rate reaches its extreme.

In order to manifest the existence of barotropic instability of tangential vortex Rossby waves in the TC, a high resolution simulated case was used to obtain the typical basic states of the TC. It is shown that the local maximum of basic vertical absolute vorticity at the RMV provides the basic configuration to vortex barotropic instability and satisfies the first necessary

condition. As the theoretical wave velocity is much slower than the tangential basic velocity in the inner core area of the TC, the positive basic radial gradient of absolute vorticity inside the RMV causes the attenuation of perturbation energy in the TC eye, while the negative basic radial gradient of absolute vorticity outside the RMV is propitious to the development of perturbation instability. Furthermore, according to the perturbation structure analysis at different WNs, it is shown that the perturbation fields at low WNs reveal the feature of VRWs, and their peaks of perturbation wind and height focus on the band area from the RMV to the outside of the RMW. This means that mesoscale barotropic instability is the main dynamic reason for the formation and development of severe storms in the eyewall.

APPENDIX A:

Estimation of Mesoscale Barotropic Instability Growth Rate

According to the nature of complex numbers, the integration equation of perturbation energy, Eq. (12), can be changed into:

$$-\int_0^{R_b} \frac{R(\overline{V}_0 - c_r)\bar{\eta}_0'}{(\overline{V}_0 - c_r)^2 + c_i^2}|\psi|^2 dR =$$

$$\int_0^{R_b} R|\psi'|^2 dr + \int_0^{R_b} R\left(\frac{k^2}{R^2}|\psi|^2\right) dR. \qquad (A1)$$

Considering the boundary condition, $\psi(R)$, can be changed to the following Fourier progression as Eq. (14), thus the first order reciprocal of stream function is:

$$\psi' = \sum_{n=1}^{\infty} \frac{n\pi}{R_b} a_n \cos \frac{n\pi R}{R_b}. \qquad (A2)$$

Using Eq. (A2) and Eq. (A3) and defining $x = n\pi r/R_b$, we can have:

$$\int_0^{R_b} R\cos^2 \frac{n\pi R}{R_b} dR = \frac{R_b^2}{n^2\pi^2} \int_0^{n\pi} x\cos^2 x\, dx$$

$$= \frac{R_b^2}{2n^2\pi^2} \int_0^{n\pi} x(1 + \cos 2x)dx$$

$$= \frac{R_b^2}{4} + \frac{R_b^2}{8n^2\pi^2} \times$$

$$\left. (2x\sin 2x + \cos 2x)\right|_0^{n\pi}$$

$$= \frac{R_b^2}{4}$$

$$\int_0^{R_b} R\sin^2 \frac{n\pi R}{R_b} dR = \int_0^{R_b} R\left(1 - \cos^2 \frac{n\pi R}{R_b}\right) dr$$

$$= \frac{R_b^2}{2} - \frac{R_b^2}{4}$$

$$= \frac{R_b^2}{4}$$

Then, the right-hand items can be respectively estimated as:

$$\int_0^{R_b} R|\psi|^2 dr = \sum_{n=1}^{\infty} a_n^2 \int_0^{R_b} \sin^2 \frac{n\pi R}{R_b} dR$$

$$= \frac{R_b^2}{4} \sum_{n=1}^{\infty} a_n^2$$

$$\int_0^{R_b} R\left(\frac{k^2}{R^2}|\psi|^2\right) dR \geqslant \frac{k^2}{R_b^2} \int_0^{R_b} R|\psi|^2 dR$$

$$= \frac{n^2}{R_b^2} \frac{R_b}{2} \int_0^{R_b} R|\psi|^2 dR$$

$$\int_0^{R_b} R|\psi'|^2 dR = \frac{R_b^2}{4} \sum_{n=1}^{\infty} \left(\frac{n\pi}{R_b}\right)^2 a_n^2 \geqslant \left(\frac{\pi}{R_b}\right)^2 \times$$

$$\frac{R_b^2}{4} \sum_{n=1}^{\infty} a_n^2 = \left(\frac{\pi}{R_b}\right)^2 \int_0^{R_b} R|\psi|^2 dr$$

So the right-hand items can be written as:

$$\int_0^{R_b} R\left(|\psi'|^2 + \frac{n^2}{R^2}|\psi|^2\right) dR$$

$$\geqslant \frac{(\pi^2 + k^2)}{R_b^2} \int_0^{R_b} R|\psi|^2 dR. \qquad (A3)$$

As

$$(\overline{V}_0 - c_r)^2 + c_i^2 \geqslant 2\left|(\overline{V}_0 - c_r)c_i\right|,$$

the left-hand item of Eq. (A1) can be estimated as:

$$-\int_0^{R_b} \frac{(\overline{V}_0 - c_r)\bar{\eta}_0'}{(\overline{V}_0 - c_r)^2 + c_i^2} R|\psi|^2 dR$$

$$\leqslant \int_0^{R_b} \left|\frac{(\overline{V}_0 - c_r)\bar{\eta}_0'}{(\overline{V}_0 - c_r)^2 + c_i^2}\right| \times$$

$$R|\psi|^2 dR \leqslant \int_0^{R_b} \frac{1}{2|c_i|}|\bar{\eta}_0'|R|\psi|^2 dR. \qquad (A4)$$

Taking Eq. (A3) and Eq. (A4) into Eq. (A1), we find:

$$\frac{(\pi^2 + k^2)}{R_b^2} \int_0^{R_b} R|\psi|^2 dR \leqslant \int_0^{R_b} \frac{1}{2|c_i|}|\bar{\eta}_0'|R|\psi|^2 dR$$

$$\leqslant \frac{1}{2|c_i|} \max_{(0,R_b)}(|\bar{\eta}_0'|) \int_0^{R_b} R|\psi|^2 dR. \qquad (A5)$$

Let us state that $\omega_{i\max}$ is the maximum possible instability growth rate of barotropic instable waves;

thus, the instable growth rate of a barotropic vortex Rossby wave is:

$$\frac{k|c_i|}{R} \leqslant \omega_{i\,\max} = \frac{k}{2R(\pi^2 + k^2)} \max_{(0,R_b)} (|\bar{\eta}_0'|) , \quad (A6)$$

which is shown in the text as Eq. (15).

APPENDIX B:

The Vortex Semicircular Theorem of Mesoscale Barotropic Instability

Taking the above expression $F = \psi/\overline{V} - c$ into Eq. (5) and adopting the f-plane approximation, we can obtain:

$$\frac{1}{R} \left[R(\overline{V}_0 - c)^2 F' \right]' -$$

$$\left[\frac{k^2}{R^2}(\overline{V}_0 - c)^2 - \frac{\overline{V}_0}{R^2}(\overline{V}_0 - c) \right] F = 0 . \quad (B1)$$

Then Eq. (17) can be obtained by multiplying the above equation by F^*, the complex conjugate of F. After integrating Eq. (B2) within the boundary, the real and imaginary parts of the equation are:

$$\int_0^{R_b} R \left[(\overline{V}_0 - c_r)^2 - c_i^2 \right] \left(\frac{k^2}{R^2}|F|^2 + |F'|^2 \right) dR -$$

$$\int_0^{R_b} \frac{\overline{V}_0^2}{R^2}(\overline{V}_0 - c_r) R |F|^2 dR = 0 \quad (B2)$$

$$c_i \left[\int_0^{R_b} R(\overline{V}_0 - c_r) \left(\frac{k^2}{R^2}|F|^2 + |F'|^2 \right) dR - \right.$$

$$\left. \frac{1}{2} \int_0^{R_b} \frac{\overline{V}_0^2}{R^2} R |F|^2 dR \right] = 0 \quad (B3)$$

Considering that instability perturbation satisfies $c_i \neq 0$, from the imaginary part of Eq. (B3) we get:

$$c_r = \left(\int_0^{R_b} R \overline{V}_0 Q dR \Big/ \int_0^{R_b} R Q dR \right) -$$

$$\left(\frac{1}{2} \int_0^{R_b} \frac{\overline{V}_0^2}{R^2} R |F|^2 dR \Big/ \int_0^{R_b} R Q dR \right) , \quad (B4)$$

where

$$Q = k^2 |F|^2 / R^2 + |F'|^2 \geqslant 0 .$$

With the result from Eq. (A3), we can have:

$$\int_0^{R_b} R Q dR = \int_0^{R_b} R \left(|F'|^2 + \frac{k^2}{R^2}|F|^2 \right) dR$$

$$\geqslant \frac{(\pi^2 + k^2)}{R_b^2} \int_0^{R_b} R |F|^2 dR . \quad (B5)$$

Therefore, after considering

$$\int_0^{R_b} (\overline{V}_0^2 |F|^2 / R) dR \geqslant 0$$

and substituting Eq. (B5) into Eq. (B4), we introduce $\overline{V}_{\min}$, $\overline{V}_{\max}$ as the minimum and maximum of basic tangential wind speed within $(0,\ R_b)$, and $\overline{\Omega}_{\max}$ as the corresponding maximum basic angular velocity. Then, the wave velocity of instable waves can be estimated as Eq. (18).

Moreover, by substituting Eq. (B4) into the real part Eq. (B2), then:

$$\int_0^{R_b} \overline{V}_0^2 R Q dR = \int_0^{R_b} R(c_r^2 + c_i^2) Q dR +$$

$$\int_0^{R_b} \frac{\overline{V}_0^2}{R^2} \overline{V}_0 R |F|^2 dR . \quad (B6)$$

Considering

$$\left(\overline{V}_0 - \overline{V}_{\min} \right) \left(\overline{V}_0 - \overline{V}_{\max} \right) \leqslant 0 ,$$

the above equation can be written as:

$$\int_0^{R_b} \left[\overline{V}_0^2 - \left(\overline{V}_{\max} + \overline{V}_{\min} \right) \overline{V}_0 + \overline{V}_{\max} \overline{V}_{\min} \right] \times$$

$$R Q dR \leqslant 0 . \quad (B7)$$

With the expression of $\overline{V}_0 \geqslant \overline{V}_{\min}$, by taking Eq. (B4) and Eq. (B6) into Eq. (B7), then:

$$\int_0^{R_b} \left[\left(c_r - \frac{\overline{V}_{\max} + \overline{V}_{\min}}{2} \right)^2 + c_i^2 - \frac{\left(\overline{V}_{\max} + \overline{V}_{\min} \right)^2}{4} - \right.$$

$$\left. \left(\frac{\overline{V}_{\max} + \overline{V}_{\min}}{2} \right) \frac{\overline{\Omega}_{\max}^2 R_b^2}{(\pi^2 + k^2)} \right] R Q dR \leqslant 0 . \quad (B8)$$

Hence, Eq. (19) can be obtained to show vortex semicircular theorem.

REFERENCES

Anthes, R. A., 1982: *Tropical Cyclones: Their Evolution, Structure and Effect.* Amer. Meteor. Soc., Boston, MA, USA, 208pp.

Charney, J. G., 1947: The dynamics of long waves in a baroclinic westerly current. *J. Meteor.*, **4**, 135–163.

Eady, E. T., 1949: Long waves and cyclone waves. *Tellus*, **1**, 33–52.

Eliassen, A., 1952: Slow thermally or frictionally controlled meridional circulation in a circular vortex. *Astrophysica Norvegica*, **5**, 19–60.

Emanuel, K. A., 1995: The behavior of a simple hurricane model using a convective scheme based on subcloud-layer entropy equilibrium. *J. Atmos. Sci.*, **52**, 3960–3968.

Frederiksen, J. S., 1979: The effects of long planetary waves on the regional cyclogenesis. *J. Atmos. Sci.*, **36**, 195–204.

Kuo, H. L., and B. C. Zhu, 1981: *Atmospheric Dynamics.* Chinese Science and Technology Press of Jiangsu, Jiangsu, China, 48pp. (in Chinese)

Liu, Y., D.-L. Zhang, and M. K. Yau, 1997: A multiscale numerical study of hurricane Andrew (1992). Part I: Explicit simulation and verification. *Mon. Wea. Rev.*, **125**, 3073–3093.

Liu, Y., D.-L. Zhang, and M. K. Yau, 1999: A multiscale numerical study of hurricane Andrew (1992). Part II: Kinematics and inner-core structures. *Mon. Wea. Rev.*, **127**, 2597–2616.

Llewellyn Smith, S. G., 1995: The influence of circulation on the stability of vortices to mode-one disturbances. *Proc. Roy. Soc. London A*, **451**, 747–755.

Macdonald, N. J., 1968: The evidence for the existence of Rossby-like waves in the hurricane vortex. *Tellus*, **20**, 138–150.

Montgmery, M. T., and R. J. Kallenbach, 1997: A theory of vortex Rossby waves and its application to spiral bands and intensity changes in hurricanes. *Quart. J. Roy. Meteor. Soc.*, **123**, 435–465.

Montgomery, M. T., and J. Enagonio, 1998: Tropical cyclogenesis via convectively forced vortex Rossby waves in a three-dimensional quasigeostrophic model. *J. Atmos. Sci.*, **55**, 3176–3207.

Montgomery, M. T., and J. L. Franklin, 1998: An assessment of the balance approximation in hurricanes. *J. Atmos. Sci.*, **55**, 2193–2200.

Nolan, D. S., and M. T. Montgomery, 2000: The algebraic growth of wavenumber one disturbances in hurricane-like vortices. *J. Atmos. Sci.*, **57**, 3514–3538.

Nolan, D. S., and M. T. Montgomery, 2002: Nonhydrostatic three-dimensional perturbations to balanced hurricane-like vortices. Part I: Linearized formulation, stability, and evolution. *J. Atmos. Sci.*, **59**, 2989–3020.

Reasor, P. D., M. T. Montgomery, F. D. Marks Jr., and J. F. Gamache, 2000: Low-wavenumber structure and evolution of the hurricane inner core observed by airborne Dual-Doppler radar. *Mon. Wea. Rev.*, **128**, 1653–1680.

Rezink, G. M., and W. K. Dewar, 1994: An analytical theory of distributed axisymmetric barotropic vortices on the beta-plane. *J. Fluid Mech.*, **269**, 301–321.

Schecter, D. A., and M. T. Montgomery, 2007: Waves in a cloudy vortex. *J. Atmos. Sci.*, **64**, 314–337.

Schubert, W. H., M. T. Montgomery, R. K. Taft, T. A. Guinn, S. R. Fulton, J. P. Kossin, and J. P. Edwards, 1999: Polygonal eyewalls, asymmetric eye contraction, and potential vorticity mixing in hurricanes. *J. Atmos. Sci.*, **56**, 1197–1223.

Smith, R. A., and M. N. Rosenbluth, 1990: Algebraic instability of hollow electron columns and cylindrical vortices. *Physical Review Letters*, **64**, 649–652.

Tepper, M. A., 1958: A theoretical model for hurricane radar bands. Preprints, *7th Conf. on Radar Meteorology*, Boston, MA, USA, Amer. Meteor. Soc., K56–K65.

Wang, Y., 2002a: Vortex Rossby waves in a numerically simulated tropical cyclone. Part I: Overall structure, potential vorticity, and kinetic energy budgets. *J. Atmos. Sci.*, **59**, 1213–1238.

Wang, Y., 2002b: Vortex Rossby waves in a numerically simulated tropical cyclone. Part II: The role in tropical cyclone structure and intensity changes. *J. Atmos. Sci.*, **59**, 1239–1262.

Willoughby, H. E., 1978a: A possible mechanism for the formation of hurricane rain bands. *J. Atmos. Sci.*, **35**, 838–848.

Willoughby, H. E., 1978b: The vertical structure of hurricane rainbands and their interaction with the mean vortex. *J. Atmos. Sci.*, **35**, 849–858.

Xu, Q., 1982: The unstable spiral inertia-gravity waves in Typhoon. *Chinese Science (B)*, **12**, 665–673. (in Chinese)

Zhang, D.-L., Y. Liu, and M. K. Yau, 2000: A multiscale numerical study of Hurricane Andrew (1992). Part III: Dynamically induced vertical motion. *Mon. Wea. Rev.*, **128**, 3772–3788.

Zhang, D.-L., Y. Liu, and M. K. Yau, 2001: A multiscale numerical study of Hurricane Andrew (1992). Part IV: Unbalanced flows. *Mon. Wea. Rev.*, **129**, 92–1107.

Zhang, D.-L., Y. Liu, and M. K. Yau, 2002: A multiscale numerical study of Hurricane Andrew (1992). Part V: Inner-core thermodynamics. *Mon. Wea. Rev.*, **130**, 2745–2763.